Formation of a Propeller Structure by a Moonlet in a Dense Planetary Ring

Shugo Michikoshi[1] and Eiichiro Kokubo[1,2]

michikoshi@cfca.jp and kokubo@th.nao.ac.jp

ABSTRACT

The Cassini spacecraft discovered a propeller-shaped structure in Saturn's A ring. This propeller structure is thought to be formed by gravitational scattering of ring particles by an unseen embedded moonlet. Self-gravity wakes are prevalent in dense rings due to gravitational instability. Strong gravitational wakes affect the propeller structure. Here, we derive the condition for formation of a propeller structure by a moonlet embedded in a dense ring with gravitational wakes. We find that a propeller structure is formed when the wavelength of the gravitational wakes is smaller than the Hill radius of the moonlet. We confirm this formation condition by performing numerical simulations. This condition is consistent with observations of propeller structures in Saturn's A ring.

Subject headings: Methods: numerical, Planets and satellites: rings

1. Introduction

A moonlet embedded in a planetary ring tends to open a gap, such as a Keeler or Encke gap, due to gravitational scattering (e.g., Lissauer et al. 1981). Conversely, viscous diffusion of ring particles tends to close a gap. If a moonlet is sufficiently large, it will form a fully circular gap, whereas a small moonlet will form only a partial gap that consists of two azimuthally aligned lobes shaped like a propeller (hereafter, we refer to this structure as a propeller). Using the viscous fluid model, Spahn & Sremčević (2000) and Sremčević et al. (2002) predicted the formation of propellers by small moonlets. The Cassini spacecraft discovered propellers in Saturn's A ring (Tiscareno et al. 2006). The moonlets are so small

[1] Center for Computational Astrophysics, National Astronomical Observatory of Japan, Osawa, Mitaka, Tokyo 181-8588, Japan

[2] Division of Theoretical Astronomy, National Astronomical Observatory of Japan, Osawa, Mitaka, Tokyo 181-8588, Japan

that they cannot be directly detected. Since the radial separation between the two lobes is related to the Hill radius of a moonlet, the size of a moonlet with a propeller can be estimated. Most of the known propellers are concentrated within narrow bands in the A ring. Moonlets with propellers have radii ranging from tens of meters to a kilometer (Tiscareno et al. 2010). The size distribution of moonlets has a steeper power-law index than that of ring particles (Tiscareno et al. 2008).

An N-body simulation is a powerful tool for studying ring dynamics where collisions and gravitational interactions play important roles. Seiß et al. (2005) and Lewis & Stewart (2009) performed N-body simulations of propeller formations. Seiß et al. (2005) considered collisions between particles but did not take into account of the self-gravity of particles. They treated the effect of self-gravity as increasing the vertical frequency (Wisdom & Tremaine 1988). They confirmed the formation of propellers and investigated the scaling law of the propeller size discussed in Sremčević et al. (2002). Lewis & Stewart (2009) included self-gravity and the size distribution of particles. They adopted a low optical depth $\tau = 0.1-0.2$, which is smaller than that of the A ring. Self-gravity causes spontaneous formation of gravitational wakes (e.g., Salo 1995; Daisaka & Ida 1999). They showed that self-gravity with a size distribution destroys the propeller structure when the ratio of the moonlet mass to the upper limit of the mass distribution is less than 30.

In this study, we perform real-scale N-body simulations of a small moonlet embedded in dense rings. The optical depth of the A ring is as high as about 0.3–0.5, while that of the B ring is larger than unity. Distinct and large gravitational wakes form in rings with large optical depths (e.g., Salo 1995; Daisaka & Ida 1999). Such large gravitational wakes may alter the structures around the embedded moonlet. We investigate the condition for propeller formation in a dense ring in which gravitational wakes are prevalent. Section 2 summarizes the calculation method. In Section 3, we present the simulation results and derive the condition for propeller formation. Section 4 consists of a discussion and a summary.

2. Calculation Method

We consider a small computational domain of a ring such that $L_x, L_y \ll a$, where L_x and L_y are the width and length of the computational domain and a is the distance from Saturn. We introduce a local Cartesian coordinate system (x, y, z). The origin revolves around Saturn with the Kepler angular velocity Ω and is located at the center of the computational domain. The x-axis is directed radially outward, the y-axis is parallel to the direction of rotation, and the z-axis is normal to the x–y plane. The computational domain has periodic boundary conditions and is surrounded by eight copies (e.g., Wisdom & Tremaine 1988; Salo

1995). The equation of motion is linearized, which is referred to as the Hill equation (e.g., Petit & Henon 1986; Nakazawa & Ida 1988). The equation of motion is integrated using a second-order leapfrog scheme with a variable time step. The sizes of the computational domain are $L_x = 10r_{\rm H}$ and $L_y = 80r_{\rm H}$, where $r_{\rm H}$ is the Hill radius of the moonlet given by $r_{\rm H} = (M/3M_{\rm s})^{1/3}a$, where M and M_s are the masses of the moonlet and Saturn, respectively.

We consider the self-gravity of ring particles and calculate it by directly summing the gravitational interactions of all pairs. We calculate not only the gravitational interactions inside the domain but also those from the surrounding copies (Salo 1995). The gravitational interactions, which are the most computationally expensive part of N-body simulations, are calculated using a programmable, special-purpose computer, GRAPE-DR (Makino et al. 2007).

The frictionless impact model for hard spheres is adopted (e.g., Richardson 1994; Daisaka & Ida 1999). In a collision, the normal component of the relative velocity is reduced by a factor ϵ, which is the restitution coefficient in the normal direction. The tangential component of the relative velocity is conserved. We adopt a restitution coefficient model that was determined by a laboratory experiment. The normal restitution coefficient is (Bridges et al. 1984)

$$\epsilon = 0.34 \min \left(\left(\frac{v_{\rm n}}{1{\rm cm/s}} \right)^{-0.234}, 1 \right), \tag{1}$$

where $v_{\rm n}$ is the normal impact velocity.

We consider the size distribution of particles. We adopt a power-law model $ndR = (R/R_0)^{-q} dR$ for $R_{\rm min} < R < R_{\rm max}$, where R is the radius of particles, R_0 is the radius for normalization, q is the power-law index for the distribution, and $R_{\rm min}$ and $R_{\rm max}$ are the minimum and maximum sizes of particles, respectively. We adopt $q = 2.8$ (Zebker et al. 1985). The density of particles is $0.5\,{\rm g/cm^3}$. The initial Toomre parameter $Q = \Omega c/3.36G\Sigma$ is set to $Q = 2$ (Toomre 1964), where c is the velocity dispersion of ring particles.

The moonlet is fixed at the origin of the coordinates. We assume that the moonlet radius is 150 m and its bulk density is $0.9\,{\rm g/cm^3}$. The semimajor axis and the Hill radius of the moonlet are a=117000 km and $r_{\rm H} = 228\,{\rm m}$, repectively. This semimajor axis corresponds to the outer region of the B ring.

3. Results

3.1. Formation and Non-Formation of Propellers

We demonstrate formation and non-formation of propellers with low and high surface density ring models. The typical minimum surface density in the B ring is estimated to be 240–480 $\mathrm{g/cm^2}$ (Robbins et al. 2010), while the surface density at its outer edge is estimated to be 30–70 $\mathrm{g/cm^2}$ (Spitale & Porco 2010). We adopt $\Sigma_0 = 62\,\mathrm{g/cm^2}$ and $414\,\mathrm{g/cm^2}$ for the low and high surface density models, respectively. The size range of particles is inferred from stellar occultation as $R_{\min} \simeq 30\,\mathrm{cm}$ and $R_{\max} \simeq 20\,\mathrm{m}$ (French & Nicholson 2000). However, due to the limitations of the available computing resources, we have to adopt the larger and smaller values respectively for $R_{\min}$ and $R_{\max}$ of $R_{\min} = 2\,\mathrm{m}$ and $R_{\max} = 10\,\mathrm{m}$ to fit the surface density to the value inferred from the density wave (e.g., Tiscareno et al. 2007). This small size range gives somewhat unrealistic dynamical optical depths of $\tau_0 = 0.18$ and 1.2 for the low and high surface density models, respectively. However, the surface density controls the basic dynamics of dense rings in which gravitational wakes develop. As is shown later, the condition for propeller formation depends on the surface density and is independent of the optical depth.

First, we show formation of a propeller in the low surface density model. Figure 1 shows a snapshot of the low surface density model at $t = 1.0T_{\mathrm{K}}$, where T_{K} is the Keplerian period $2\pi/\Omega$. A propeller-shaped feature is clearly visible in the weak gravitational wakes. The surface density decreases considerably in the two lobes downstream of the moonlet. They are aligned in the orbital direction and are symmetric about the moonlet. The minimum density in the propeller is located at about $x = \pm 2r_{\mathrm{H}} = 456\,\mathrm{m}$ and $y = \mp 4\,\mathrm{km}$ (Seiß et al. 2005). The radial separation between the two lobes is about $4r_{\mathrm{H}}$ and the radial width of a single lobe is about $2r_{\mathrm{H}}$ (Spahn & Sremčević 2000; Sremčević et al. 2002; Seiß et al. 2005; Tiscareno et al. 2008; Lewis & Stewart 2009). The length of the lobe in the azimuthal direction is about 5 km. We define the propeller region as the region of $-3 < x/r_{\mathrm{H}} < -2$ and $15 < y/r_{\mathrm{H}} < 20$, which is the typical region of a propeller lobe (Spahn & Sremčević 2000; Sremčević et al. 2002; Seiß et al. 2005; Lewis & Stewart 2009). The ratio of the time-averaged surface density in the propeller region to the initial surface density $\bar{\Sigma}/\Sigma_0$ is 0.17.

Next, we demonstrate non-formation of a propeller in the high surface density model. Numerical simulations reveal that a strong wake structure due to gravitational instability forms for this parameter (Salo 1995; Daisaka & Ida 1999). As expected, until $t = 0.5T_{\mathrm{K}}$, gravitational instability occurs and wakes start forming. Figure 2 shows a snapshot of the high surface density model at $t = 4.0T_{\mathrm{K}}$. Strong gravitational wakes form and no propeller structure is clearly observed. The ratio of the time-averaged surface density in the propeller region to the initial surface density $\bar{\Sigma}/\Sigma_0$ is 0.41. The gravitational wakes seem to be almost unaffected by the moonlet. The typical distance between wakes is approximated by the critical wavelength of gravitational instability $\lambda_{\rm cr} = 4\pi^2 G\Sigma/\Omega^2$, where Σ is the ring surface density (e.g., Julian & Toomre 1966; Salo 1995). In the high surface density model, the typical distance between wakes is $\lambda_{\rm cr} = 459$ m, which is larger than the Hill radius of the moonlet.

3.2. Condition for Propeller Formation

The numerical simulation results indicate that propeller formation depends on the surface density. Below, we derive the formation condition for propellers and confirm its validity by performing N-body simulations.

The clumps in gravitational wakes typically have a mass of $\sim \Sigma\lambda_{\rm cr}^2$. If the clump mass is greater than the moonlet mass M, the gravitational wakes may not be affected by gravitational scattering due to the moonlet. Comparing the clump mass with the moonlet mass, we obtain the following condition for propeller formation

$$\lambda_{\rm cr} \lesssim r_{\rm H}. \tag{2}$$

Note that this condition can also be derived by comparing the typical velocity due to scattering by the moonlet with the velocity dispersion of ring particles (Lewis & Stewart 2009). If the velocity dispersion of particles exceeds the Hill velocity $r_{\rm H}\Omega$, which is a typical velocity due to scattering by the moonlet, the gravitational wake should be almost unaffected by the moonlet. The velocity dispersion of ring particles c is determined by $Q = 2$ (Salo 1995; Daisaka & Ida 1999). Thus, the ratio of c to $r_{\rm H}\Omega$ is about $\lambda_{\rm cr}/r_{\rm H}$.

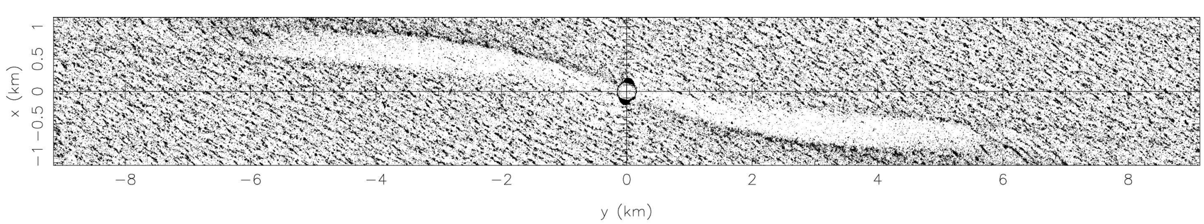

Fig. 1.— Snapshot of low surface density model at $t = 1.0T_{\rm K}$. The initial surface density is $\Sigma_0 = 62{\rm g/cm}^2$. The circle at the center of the computational box is the moonlet. A propeller structure is visible around the moonlet.

Using the moonlet radius and the ring surface density, Equation (2) can be rewritten as

$$\begin{aligned}\Sigma < \Sigma_{\rm cr} &\equiv C\left(\frac{M_{\rm s}^2\rho R^3}{144\pi^5 a^6}\right)^{1/3} \\ &= 167\,{\rm g/cm^2}\left(\frac{C}{1.5}\right)\left(\frac{a}{1.3\times10^5\,{\rm km}}\right)^{-2}\left(\frac{\rho}{0.9\,{\rm g/cm^3}}\right)^{1/3}\left(\frac{R}{100\,{\rm m}}\right) \qquad (3)\end{aligned}$$

where C is the non-dimensional constant of order unity (see discussion below) and ρ and R are respectively the density and radius of the moonlet.

To check the validity of this condition, we perform N-body simulations for various Σ and R. To investigate a wide range of Σ, we adopt equal-sized (10 m) ring particles, which reduces the number of particles. The density of particles is 0.5g/cm^3. We assume that the restitution coefficient is constant at $\epsilon = 0.1$. The moonlet density is 0.7g/cm^3.

We perform 25 simulations with different ring surface densities and moonlet radii. We vary the moonlet radius from 60 m to 250 m and the surface density from $\Sigma = 133\,{\rm g/cm^2}$ to $\Sigma = 670\,{\rm g/cm^2}$. The ratio of the radius to the Hill radius is 0.64. The simulation time is $6T_{\rm K}$. We consider that a propeller forms if $\bar{\Sigma}/\Sigma_0 < 0.2$ in the propeller region. We confirmed that a propeller-shaped structure is clearly observed when this condition is satisfied. If this condition is not satisfied, no distinct steady propeller structure is observed (although the ring particles are affected by the moonlet to some extent). Figure 3 summarizes the results. It clearly shows that Equation (3) is consistent with the simulation results. We find that $C = 1.68$ explains the $\bar{\Sigma}/\Sigma_0 = 0.2$ boundary well. We also find that C is approximately proportional to the boundary value of $\bar{\Sigma}/\Sigma_0$.

For a moonlet with a radius of 150 m and a density of 0.9 g/cm^3, the critical surface density is 308 g/cm^2. In the low surface density model, the surface density is 62 g/cm^2, which is smaller than the critical value. In this case, a propeller is clearly observed. On the other hand, in the high surface density model, since the surface density is 414g/cm^2, which is

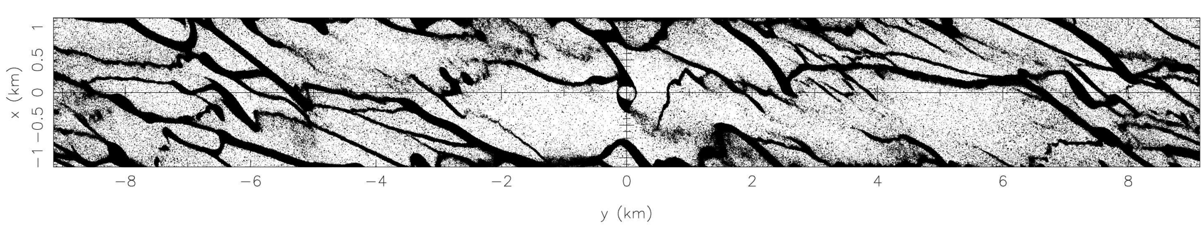

Fig. 2.— Same as for Figure 1, but for the high surface density model with $\Sigma = 414$ g/cm^2 at $t = 4.0T_{\rm K}$. Strong gravitational wakes form and a propeller structure is not clearly observed.

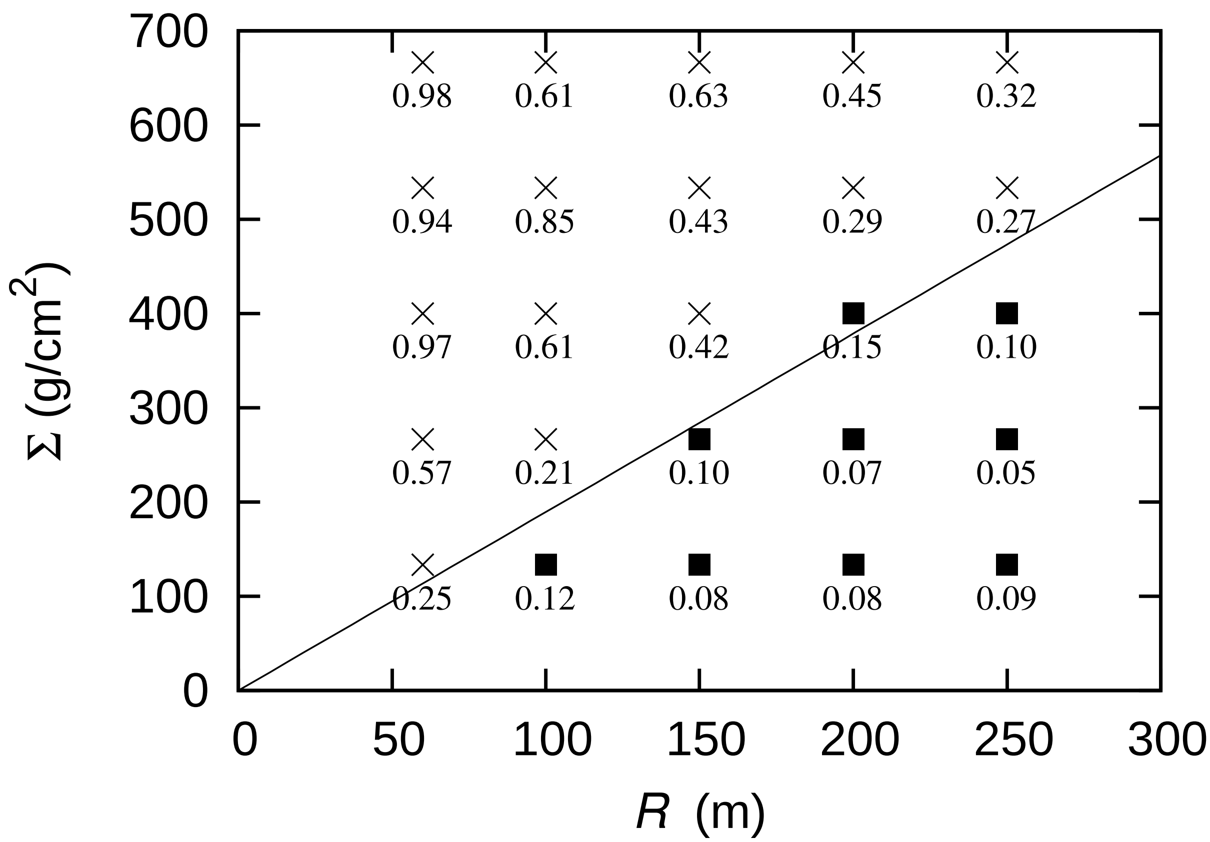

Fig. 3.— Condition for propeller formation in Saturn's B ring in the R-Σ plane. Filled squares denote models in which clear propellers form and crosses denote models in which no propellers form. We show the ratio of the time-averaged surface density in the propeller region to the initial surface density $\bar{\Sigma}/\Sigma_0$ at each point. The solid line indicates the condition for propeller formation estimated by Equation (3) with $C = 1.68$.

greater than the critical value, a gravitational wake prevails over a propeller. Consequently, no propeller is observed.

Figure 4 shows the critical surface density plotted as a function of distance from Saturn for moonlets with $\rho = 0.9\,\mathrm{g/cm^3}$ and $R = 10$, 30, 100, and 300 m. Since $\lambda_{\rm cr}$ increases with a faster than $r_{\rm H}$, $\Sigma_{\rm cr}$ decreases with increasing a. The typical surface density in the A ring is about $40\mathrm{g/cm^2}$ (e.g., Esposito et al. 1983; Tiscareno et al. 2008). Assuming $\rho = 0.9\mathrm{g/cm^3}$, we obtain the critical moonlet radius for propeller formation to be 20 m. Known moonlets with propellers have radii ranging from 20 m to a kilometer (Tiscareno et al. 2008, 2010). Equation (3) is consistent with this observational data.

Note that this condition is not applicable to rings with low surface densities in which gravitational wakes do not develop well. In this case, gravitational scattering of individual particles is important and the condition discussed in Lewis & Stewart (2009) should be applicable, namely that propeller formation is controlled by the ratio of the maximum ring particle mass to the moonlet mass.

4. Summary and Discussion

We have performed local N-body simulations to investigate the formation of a propeller by a moonlet. By performing real-scale simulations, we demonstrated that in the B ring a moonlet with radius $R = 150\,\mathrm{m}$ forms a propeller in a low surface density ring ($60\,\mathrm{g/cm^2}$), whereas it does not in a high surface density ring ($414\,\mathrm{g/cm^2}$) in which the ring dynamics are dominated by gravitational wakes. These results indicate that propeller formation depends on the surface density. Comparing the moonlet mass with the typical mass of a gravitational wake, we derived the condition for propeller formation that the characteristic length of the gravitational wakes given by the critical wavelength for gravitational instability be shorter than the Hill radius of the moonlet, $\lambda_{\rm cr} \lesssim r_{\rm H}$. We confirmed this by N-body simulations. In a ring with gravitational wakes, the characteristic length of wakes is more important than the size of individual ring particles since a wake is a coherent structure. Our condition is consistent with observations of propellers in Saturn's A ring which revealed observational signatures of gravitational wakes (e.g., French et al. 2007).

The Cassini spacecraft recently discovered a new putative "moonlet" in the B ring (S/2009 S1) (Porco 2009). The diameter of S/2009 S1 is inferred to be 300 m if it is orbiting in the same plane as the ring particles. Its radial distance from the center of Saturn is 116,914 km, which is at the outer edge of the B ring (Spitale & Porco 2010). Surprisingly, no propeller was observed around S/2009 S1. For S/2009 S1, the critical surface density

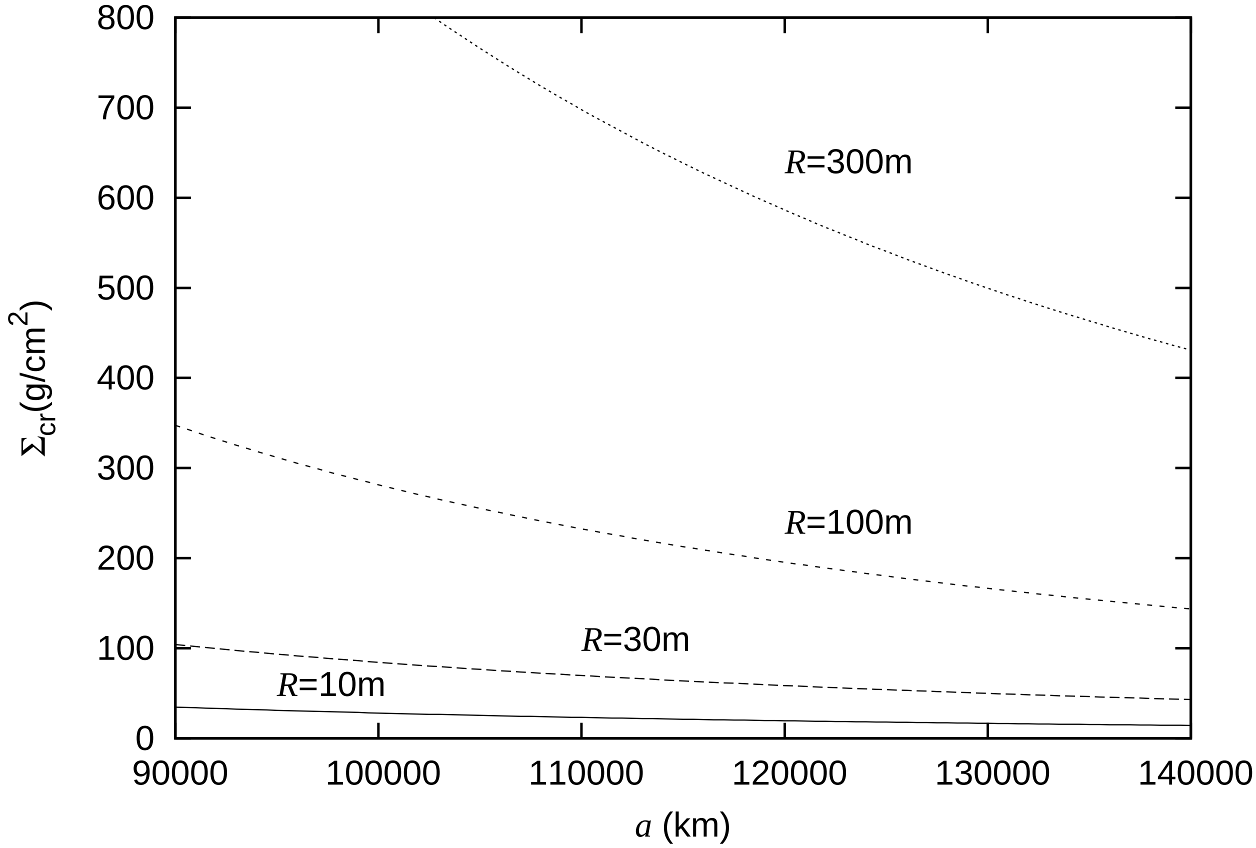

Fig. 4.— Critical surface density as a function of distance from Saturn for moonlets with $R = 10\,\mathrm{m}$ (solid curve), $30\,\mathrm{m}$ (dashed curve), $100\,\mathrm{m}$ (short dashed curve), and $300\,\mathrm{m}$ (dotted curve). The moonlet density is $0.9\,\mathrm{g/cm^3}$.

for propeller formation is estimated to be $\Sigma_{\rm cr} = 308{\rm g/cm}^2$, which is higher than the typical surface density of the outer edge of the B ring. This suggests two possibilities: the surface density around S/2009 S1 is locally high enough to prevent propeller formation or S/2009 S1 is not a moonlet but a transient feature such as meteoroid impact or temporary clumps. Further observation is necessary to determine the nature of S/2009 S1.

For simplicity, we assumed that the moonlet is fixed. If the moonlet can move, the moonlet will be scattered by gravitational wakes, which leads to stochastic change in the moonlet orbit (Lewis & Stewart 2009). This random motion of the moonlet may hinder propeller formation. It is important to determine the shape of propeller structures to interpret observations. The shape may depend on various ring parameters such as the ring viscosity and the size distribution of ring particles. We intend to investigate these problems in a subsequent study.

Observations of propeller structures reveal bright regions rather than low-density features such as a propeller gap (Sremčević et al. 2007). However, the implied density enhancement near the moonlet has not been observed in numerical simulations (Lewis & Stewart 2009). One possible explanation for the brightness enhancement is collisional debris released from ring particles (Sremčević et al. 2007). Gravitational scattering of ring particles by the moonlet increases the impact velocity between ring particles. Thus, debris may be released from ring particles in the vicinity of the moonlet in high-velocity collisions, which increases the reflectivity. As shown in Section 3.2, the condition for propeller gap formation is equivalent to that the Hill velocity of the moonlet $r_{\rm H}\Omega$ is higher than the velocity dispersion of ring particles. Therefore, it may be applicable to the condition for local debris enhancement. We intend to study this in the future.

We wish to thank Joseph A. Burns for stimulating discussions on the observations of propellers by the Cassini spacecraft. E. K. is grateful to the Isaac Newton Institute for Mathematical Sciences for its hospitality during his visit at the beginning of this study. The numerical calculations were performed on the GRAPE system at the Center for Computational Astrophysics of the National Astronomical Observatory of Japan.

REFERENCES

Bridges, F. G., Hatzes, A., & Lin, D. N. C. 1984, Nature, 309, 333

Colwell, J. E., Esposito, L. W., Sremčević, M., Stewart, G. R., & McClintock, W. E. 2007, Icarus, 190, 127

Colwell, J. E., Nicholson, P. D., Tiscareno, M. S., Murray, C. D., French, R. G., & Marouf, E. A. 2009, 375

Daisaka, H. & Ida, S. 1999, Earth, Planets, and Space, 51, 1195

Esposito, L. W., Ocallaghan, M., & West, R. A. 1983, Icarus, 56, 439

French, R. G. & Nicholson, P. D. 2000, Icarus, 145, 502

French, R. G., Salo, H., McGhee, C. A., & Dones, L. 2007, Icarus, 189, 493

Julian, W. H. & Toomre, A. 1966, ApJ, 146, 810

Lewis, M. C. & Stewart, G. R. 2009, Icarus, 199, 387

Lissauer, J. J., Shu, F. H., & Cuzzi, J. N. 1981, Nature, 292, 707

Makino, J., Hiraki, K., & Inaba, M. 2007, Proceedings of the 2007 ACM/IEEE conference, 1

Nakazawa, K. & Ida, S. 1988, Progress of Theoretical Physics Supplement, 96, 167

Petit, J.-M. & Henon, M. 1986, Icarus, 66, 536

Porco, C. C. 2009, IAU Circ., 9091, 1

Richardson, D. C. 1994, MNRAS, 269, 493

Robbins, S. J., Stewart, G. R., Lewis, M. C., Colwell, J. E., & Sremčević, M. 2010, Icarus, 206, 431

Salo, H. 1995, Icarus, 117, 287

Seiß, M., Spahn, F., Sremčević, M., & Salo, H. 2005, Geophys. Res. Lett., 32, 11205

Spahn, F. & Sremčević, M. 2000, A&A, 358, 368

Spitale, J. N. & Porco, C. C. 2010, AJ, 140, 1747

Sremčević, M., Schmidt, J., Salo, H., Seiß, M., Spahn, F., & Albers, N. 2007, Nature, 449, 1019

Sremčević, M., Spahn, F., & Duschl, W. J. 2002, MNRAS, 337, 1139

Tiscareno, M. S., Burns, J. A., Hedman, M. M., & Porco, C. C. 2008, AJ, 135, 1083

Tiscareno, M. S., Burns, J. A., Hedman, M. M., Porco, C. C., Weiss, J. W., Dones, L., Richardson, D. C., & Murray, C. D. 2006, Nature, 440, 648

Tiscareno, M. S., Burns, J. A., Nicholson, P. D., Hedman, M. M., & Porco, C. C. 2007, Icarus, 189, 14

Tiscareno, M. S., Burns, J. A., Sremčević, M., Beurle, K., Hedman, M. M., Cooper, N. J., Milano, A. J., Evans, M. W., Porco, C. C., Spitale, J. N., & Weiss, J. W. 2010, ApJ, 718, L92

Toomre, A. 1964, ApJ, 139, 1217

Wisdom, J. & Tremaine, S. 1988, AJ, 95, 925

Zebker, H. A., Marouf, E. A., & Tyler, G. L. 1985, Icarus, 64, 531